Plasma Instabilities

K. G. McClements

United Kingdom Atomic Energy Authority, Culham Campus, Abingdon, OX14 3DB, Oxon, United Kingdom

Abstract

An introductory tutorial on plasma stability theory is presented, focussing on application of the normal mode method to the linearised form of the magnetohydodynamic (MHD), Vlasov and Maxwell equations. Following an illustration of how this method can be applied to a simple mechanical problem, single-fluid stability theory is demonstrated for the case of two spatially separated unmagnetised fluids in the presence of an external force (the Rayleigh-Taylor instability) and a cylindrical magnetised plasma (sausage and kink instabilities). This is followed by a somewhat more heuristic description of two types of instability that play important roles in toroidal plasmas: ballooning modes and tearing modes. The remainder of the article is on two-fluid and kinetic instabilities, starting with the two-stream (Buneman) instability and progressing to its kinetic analogue, the electrostatic bump-in-tail instability, with a detailed discussion of inverse Landau damping, the mechanism that drives it. The article ends with a discussion of how kinetic stability theory can be extended to electromagnetic fluctuations, and the application of this analysis to ion cycloton emission in magnetised plasmas.

1 Introduction

Setting time derivatives equal to zero in the fluid or kinetic equations describing a plasma, we can look for steady-state (equilibrium) solutions of those equations. However the existence of such solutions does not guarantee that they are stable. Indeed plasma configurations are often unstable, which means that small perturbations of the equilibrium state grow in time. They subsequently either reach a steady amplitude, at a level determined by one or more nonlinear effects or, in the case of laboratory experiments, can sometimes cause the plasma to disrupt, with a complete loss of confinement. Another important point to understand is that plasma modes can be linearly stable but nonlinearly unstable. For example, *neoclassical tearing modes* are typically damped at low amplitude (that is, in the linear regime) but can grow if a perturbation of sufficiently large size, in the form of a magnetic island, is already present in the plasma. However in this paper the emphasis will be on linear stability, since this case is generally simpler to analyse.

The concept of linear instability can be illustrated using a simple mechanical example. Consider a ball in a gravitational field which is slightly displaced from its equilibrium position at the top of a hemispherical hill of height h, as shown in Fig. 1. If the ball is displaced a distance s along the surface of the hill its equation of motion

is

$$\ddot{s} = g \sin\theta, \tag{1}$$

where g is acceleration due to gravity and the angle θ expressed in radians is equal to s/h. If we consider small displacements of the ball, such that $s \ll h$, we can use the expansion $\sin\theta = \theta - \theta^3/3! + ...$, and retain only the first term, so that Eq. (1) reduces to the linear equation

$$\ddot{s} = \frac{g}{h} s. \tag{2}$$

Looking for solutions of the form $s \propto e^{-i\omega t}$ where $\omega \equiv \omega_r + i\gamma$ is a complex number, so that ω_r is an oscillation frequency while γ is a growth or damping rate, depending on its sign, we immediately obtain

$$\omega^2 = -\frac{g}{h}. \tag{3}$$

This indicates that $\omega = \pm i(g/h)^{1/2}$, and hence that all solutions of Eq. (2) are either exponentially increasing in time or exponentially decaying. In general the complete solution for a specified initial state is a linear combination of the growing and decaying solutions, with the growing solution becoming dominant for $t \gg (h/g)^{1/2}$. There is an equilibrium solution of Eq. (1), $s = 0$, but it is intuitively obvious that this will never be realised in practice. Mathematically, the system diverges exponentially in time from the equilibrium solution in the presence of infinitesimal perturbations.

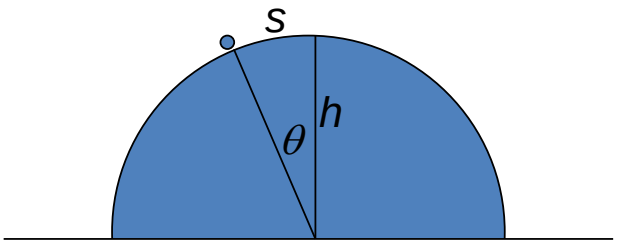

Fig. 1 Ball rolling down a hill: a mechanical analogue of plasma instability.

It will be demonstrated in this article that exactly the same methodology can be applied to the problem of plasma stability. In the greater part of the paper (Section 2), stability will be considered in the framework of a single-fluid plasma model, starting with the Rayleigh-Taylor instability (Section 2.1), which is relatively straightforward to study because it can occur in the absence of a magnetic field. A brief discussion of the linearised magnetohydrodynamic (MHD) equations (Section 2.2) is then followed by a detailed analysis of the ideal MHD instabilities of a cylindrical magnetised plasma (Section 2.3), and more qualitative treatments of pressure-driven and resistive instabilities in toroidal plasmas (Sections 2.4 and 2.5). Section 3 is concerned with instabilities that require either a two-fluid or a kinetic description. We begin with current-driven electrostatic instabilities (Sections 3.1 and 3.2) and progress to electromagnetic instabilities driven by non-Maxwellian particle velocity distributions (Section 3.3).

2 Magnetohydrodynamic instabilities

The MHD equations for a plasma subject to a gravitational acceleration (or other prescribed force per unit mass) $\boldsymbol{g}$ can be written in the form

$$\frac{\partial \rho}{\partial t} + \nabla \cdot (\rho \boldsymbol{v}) = 0, \tag{4}$$

$$\rho \left[\frac{\partial \boldsymbol{v}}{\partial t} + (\boldsymbol{v} \cdot \nabla \boldsymbol{v}) \right] = \boldsymbol{j} \times \boldsymbol{B} - \nabla p + \rho \boldsymbol{g}, \tag{5}$$

$$\boldsymbol{E} + \boldsymbol{v} \times \boldsymbol{B} = \eta \boldsymbol{j}, \tag{6}$$

$$\nabla \times \boldsymbol{E} = -\frac{\partial \boldsymbol{B}}{\partial t}, \tag{7}$$

$$\nabla \times \boldsymbol{B} = \mu_0 \boldsymbol{j}, \tag{8}$$

where ρ is mass density, $\boldsymbol{v}$ is fluid velocity, p is pressure, $\boldsymbol{E}$ and $\boldsymbol{B}$ denote electric and magnetic fields, $\boldsymbol{j}$ is current density, η is electrical resistivity (often assumed to be constant in space and time) and μ_0 is free space permeability. Physically, Eq. (4) expresses mass conservation. The momentum equation [Eq. (5)] includes the total time derivative operator $d/dt = \partial/\partial t + \boldsymbol{v} \cdot \nabla$ which is required for fluid motion. The current in the plasma is linked by the resistivity to the electric field in the plasma rest frame $\boldsymbol{E} + \boldsymbol{v} \times \boldsymbol{B}$ by Ohm's law [Eq. (6)]. Faraday's law of induction [Eq. (7)] and Ampère's law [Eq. (8)] complete the set. An additional equation is required to close the system, since, in the most general case, there are fourteen dependent variables (ρ, p, $\boldsymbol{v}$, $\boldsymbol{E}$, $\boldsymbol{B}$, $\boldsymbol{j}$) and Eqs. (4-8) comprise thirteen scalar equations. As demonstrated later in this section, the additional equation is generally obtained by either assuming that the plasma is incompressible or by making a simplifying assumption regarding energy transport.

Specific MHD equilibria are obtained by solving the steady-state form ($\partial/\partial t = 0$) of Eqs. (4-8). There are three techniques which can then be used to determine the stability of these equilibria. One of these is based on the *energy principle*, which requires calculation of the change in potential energy δW that would be caused by a perturbation from equilibrium. Positive and negative values of δW indicate that the system is respectively stable and unstable, but this approach does not in general yield expressions for growth rates or spatial information on the development of any instability. Alternatively one may use the *normal mode method*: the equations are first linearised, and solutions for perturbed quantities varying in time as $\exp(-i\omega t)$ are sought, $\omega = \omega_r + i\gamma$ being a complex frequency whose permissible values are determined by boundary conditions. As in the case of the ball rolling down a hill, the existence of any positive values of γ implies exponential growth of the perturbation and hence instability. Finally, one may employ the *initial value* approach whereby the time-dependent equations are solved directly (usually numerically), starting from specified initial conditions. The emphasis in this article will be on the normal mode method.

2.1 The Rayleigh-Taylor instability

Instability occurs when a dense fluid is supported against gravity by a less dense fluid (Rayleigh 1883) or, equivalently, when a dense fluid is decelerated by an adjacent less dense fluid. This scenario, which arises in inertially-confined fusion plasmas and also astrophysical plasmas (supernovae), can be used to illustrate the normal mode method without the complicating presence of a magnetic field.

The fluid is assumed to be incompressible, meaning that the total (advective) time derivative of the density is zero:

$$\frac{\partial \rho}{\partial t} + \boldsymbol{v} \cdot \nabla \rho = 0. \tag{9}$$

It follows from Eqs. (9) and (4) that in this case the flow must be divergence-free,

$$\nabla \cdot \boldsymbol{v} = 0. \tag{10}$$

We assume that there is no magnetic field, so that the momentum equation [Eq. (5)] reduces to

$$\rho \left[\frac{\partial \boldsymbol{v}}{\partial t} + (\boldsymbol{v} \cdot \nabla \boldsymbol{v}) \right] = -\nabla p + \rho \boldsymbol{g}. \tag{11}$$

Denoting equilibrium quantities by subscript zero, and assuming that there are no equilibrium flows (i.e. $\boldsymbol{v}_0 = 0$), we note that the steady-state form of Eq. (11) is the hydrostatic equation

$$\nabla p_0 = \rho_0 \boldsymbol{g}. \tag{12}$$

The stability of Eqs. (10) and (11) to small perturbations is examined by writing $\rho = \rho_0 + \rho_1$, $p = p_0 + p_1$ and $\boldsymbol{v} = \boldsymbol{v}_1$. The perturbations with subscript 1 are assumed, in the linear approximation, to be small in the sense that we can neglect all quantities involving products of ρ_1, p_1, $\boldsymbol{v}_1$ and their derivatives. Subtracting Eq. (12) from the linearised form of Eq. (11) we obtain

$$\rho_0 \frac{\partial \boldsymbol{v}_1}{\partial t} = -\nabla p_1 + \rho_1 \boldsymbol{g}, \tag{13}$$

and Eqs. (9) and (10) have the linearised forms

$$\frac{\partial \rho_1}{\partial t} = \boldsymbol{v}_1 \cdot \nabla \rho_0, \tag{14}$$

$$\nabla \cdot \boldsymbol{v}_1 = 0. \tag{15}$$

We now consider the case of a uniform equilibrium in the plane perpendicular to the gravitational force per unit mass $\boldsymbol{g}$, which is balanced by a pressure gradient in the opposite direction; the coordinate system is shown in Fig. 2. This equilibrium is perturbed by a one-dimensional wave propagating with wavevector $\boldsymbol{k} = (k_x, 0, k_z)$ in the plane normal to $\boldsymbol{g}$. Without loss of generality, we may set $k_x = 0$ and $k_z = k$, so that the space and time dependence of the perturbations to ρ, p and $\boldsymbol{v}$ is of the form $\exp[i(kz - i\omega t)]$. Perturbations with an arbitrary dependence on z can always be expressed as a sum over Fourier components of this form.

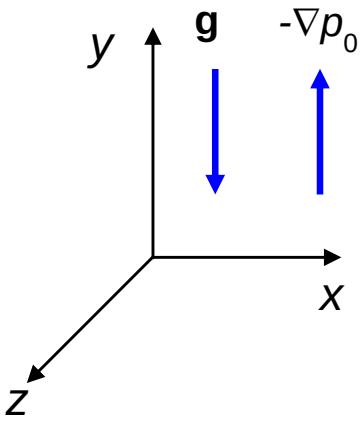

Fig. 2 Equilibrium forces and coordinate system used to describe Rayleigh-Taylor instability.

Putting $\boldsymbol{g} = (0, -g, 0)$, substituting the assumed form of the perturbations into the linearised equations [Eqs. (13-15)], and writing the y and z components of the momentum equation separately, we obtain four scalar equations for ρ_1, p_1, v_{1y} and v_{1z}:

$$-i\omega\rho_0 v_{1y} = -\frac{dp_1}{dy} - \rho_1 g, \tag{16}$$

$$-i\omega\rho_0 v_{1z} = -ikp_1, \tag{17}$$

$$-i\omega\rho_1 = -v_{1y}\frac{d\rho_0}{dy}, \tag{18}$$

$$\frac{dv_{1y}}{dy} + ikv_{1z} = 0. \tag{19}$$

We may use Eqs. (16-19) to eliminate p_1, ρ_1 and v_{1z}, leaving a single second order differential equation for v_{1y}:

$$\frac{d}{dy}\left(\rho_0\frac{dv_{1y}}{dy}\right) - k^2\left(\rho_0 + \frac{g}{\omega^2}\frac{d\rho_0}{dy}\right)v_{1y} = 0. \tag{20}$$

Eq. (20) poses a classic eigenvalue problem: for a prescribed density profile $\rho_0(y)$ and prescribed boundary conditions on v_{1y} in the y domain, solutions of this equation exist only for specific values of ω. We will now determine these values of ω for the simplest nontrivial case, that of two fluids in contact at $y = 0$ with uniform equilibrium densities $\rho_0 = \rho_a$ $(y > 0)$ and $\rho_0 = \rho_b$ $(y < 0)$. Within each fluid, the equilibrium density gradient is zero, so that, dropping the subscript "1" on perturbed quantities, Eq. (20) reduces to

$$\frac{d^2v_y}{dy^2} = k^2 v_y. \tag{21}$$

If the fluids labelled a and b are of infinite extent in the positive and negative y directions respectively, the only physically acceptable solutions of this equation for $y > 0$ (v_{y+}) and $y < 0$ (v_{y-}) have the form

$$v_{y\pm}(y) = v_y(0) \exp(\mp ky) . \tag{22}$$

The constant $v_y(0)$ must be common to the two solutions, to ensure that v_y is continuous across the boundary; this is required by the incompressibility equation [Eq. (19)]. Note however that dv_y/dy itself is *dis*continuous at $y = 0$. Having identified the form of the solution in each fluid, in order to progress we need to match these solutions across the boundary between them. We achieve this by returning to Eq. (20) and integrating it through $y = 0$ from $-\epsilon$ to $+\epsilon$ where $\epsilon \ll 1/k$, so that $v_y(y)$ in this range can be approximated by the constant value $v_y(0)$. We thus obtain

$$\rho_0 \frac{dv_y}{dy}\bigg|_{-\epsilon}^{+\epsilon} - \frac{k^2 g}{\omega^2}\rho_0\bigg|_{-\epsilon}^{+\epsilon} v_y(0) = \epsilon k^2(\rho_a + \rho_b)v_y(0). \tag{23}$$

In the limit $\epsilon \to 0$, the right hand side of this equation vanishes and we can re-write the left hand side as

$$\rho_a \left(\frac{dv_y}{dy}\right)_{0^+} - \rho_b \left(\frac{dv_y}{dy}\right)_{0^-} - \frac{k^2 g}{\omega^2}(\rho_a - \rho_b)v_y(0) = 0, \tag{24}$$

where the subscripts 0^+ and 0^- mean that dv_y/dy is evaluated as $y \to 0$ through, respectively, positive and negative values. Substituting the solution given by Eq. (21) into Eq. (23), cancelling the resulting common factor $v_y(0)$ and rearranging, we obtain the dispersion relation

$$\omega^2 = kg\frac{\rho_b - \rho_a}{\rho_b + \rho_a}. \tag{25}$$

This result links the complex frequency ω to the real wavenumber k of the perturbation. Recalling the definition of ω, we note that if $\omega^2 < 0$ we have $\omega = \pm i\gamma$ where γ is real and positive. In such cases one root of the dispersion relation gives $v_y \sim \exp(\gamma t)$, indicating instability. From Eq. (25) we infer that the equilibrium is stable if $\rho_a < \rho_b$ and unstable if $\rho_a > \rho_b$, so instability occurs if $\boldsymbol{g}$ (or ∇p_0) is directed from the heavy fluid to the light fluid. This is the Rayleigh-Taylor instability.

In plasmas that are susceptible to this instability, the effective gravity generally arises from the fact that a dense fluid is decelerating into a less dense one. Transforming from an inertial frame to one that is accelerating at a rate $\partial \boldsymbol{v}_0/\partial t$, one finds that there is an inertial force per unit mass $\boldsymbol{g} = -\partial \boldsymbol{v}_0/\partial t$ in the accelerating frame (see e.g. Thyagaraja and McClements 2009). Thus, a deceleration in the negative y-direction produces an effective force in that direction, as shown in Fig. 2.

The Rayleigh-Taylor instability often occurs during the laser-driven implosion of an inertially confined fusion plasma (Shiau et al. 1974). In this case the effective gravity is enormous, typically of order 10^{14} ms^{-2},[1] while $\rho_a \gg \rho_b$ so that the density contrast

[1] To put this figure into perspective, it is considerably higher than the typical acceleration at the surfaces of neutron stars, whose gravitational fields are among the strongest in the Universe outside the event horizons of black holes.

factor $(\rho_a - \rho_b)/(\rho_a + \rho_b)$ is close to unity, and perturbations with a wavelength λ of, say, $100\,\mu$m have a growth time

$$\tau = \frac{1}{\gamma} = \left(\frac{\lambda}{2\pi g} \frac{\rho_a + \rho_b}{\rho_a - \rho_b} \right)^{1/2} \sim 1\,\mathrm{ns}. \tag{26}$$

This is a typical timescale in inertially-confined fusion plasma experiments. A similar phenomenon is believed to occur during supernova explosions in stars, when expanding dense core material is decelerated by less dense outer regions (Remington et al. 1997). In this case the effective gravity is much less extreme, of order $10^2\,\mathrm{ms}^{-2}$, and the density contrast is also smaller, typically $(\rho_a - \rho_b)/(\rho_a + \rho_b) \sim 1/4$. From Eq. (26), we find that these figures yield a growth time of about an hour for $\lambda = 10^7\,\mathrm{km}$, which is a typical stellar lengthscale. Two-dimensional hydrodynamic simulations of supernova SN1987A show filamentary structures developing on timescales of this order (Remington et al. 1997).

Since most plasmas are embedded in magnetic fields it is important to examine the influence of such fields on the Rayleigh-Taylor instability. Here we will consider, for simplicity, the case of a uniform equilibrium field $\boldsymbol{B}_0$ in the z-direction, i.e. the direction of wave propagation, and zero resistivity ($\eta = 0$). Since $\boldsymbol{B}_0$ is curl-free there is no equilibrium current and so the linearised momentum equation that follows from Eq. (5) for an electrically conducting single fluid is

$$\rho_0 \frac{\partial \boldsymbol{v}_1}{\partial t} = -\nabla p_1 + \rho_1 \boldsymbol{g} + \boldsymbol{j}_1 \times \boldsymbol{B}_0. \tag{27}$$

Here $\boldsymbol{j}_1 = \nabla \times \boldsymbol{B}_1/\mu_0$ and the magnetic field perturbation $\boldsymbol{B}_1$ satisfies the linearised ideal MHD induction equation, which follows from Eqs. (6-7) in the limit $\eta \to 0$:

$$\frac{\partial \boldsymbol{B}_1}{\partial t} = \nabla \times (\boldsymbol{v}_1 \times \boldsymbol{B}_0). \tag{28}$$

For the case of two uniform fluids, a procedure similar to the one used previously leads to the dispersion relation

$$\omega^2 = kg \frac{\rho_b - \rho_a}{\rho_b + \rho_a} + \frac{2k^2 B_0^2}{\mu_0(\rho_b + \rho_a)}. \tag{29}$$

We note first that ω^2 is still real so that, as before, we either have an undamped oscillation ($\omega^2 > 0$) or non-oscillatory growth and damping ($\omega^2 < 0$). However the additional term due to the magnetic field is always positive and hence stabilising. Physically this arises from the fact that $\boldsymbol{B}_1$ has a component orthogonal to $\boldsymbol{B}_0$. The perturbed magnetic field lines are thus bent; additional free energy is required for bending to occur, and therefore the instability grows at a slower rate. Putting $\omega = i\gamma$ we can write Eq. (28) as

$$\gamma^2 = \gamma_0^2 - k^2 c_A^2, \tag{30}$$

where $\gamma_0 = [kg(\rho_a - \rho_b)/(\rho_a + \rho_b)]^{1/2}$ is the growth rate in the absence of the magnetic field and $c_A = B_0/\sqrt{\mu_0(\rho_a + \rho_b)/2}$ is the Alfvén speed corresponding to the mean

density of the two fluids. Since the wavevector $\boldsymbol{k}$ is parallel to $\boldsymbol{B}_0$, a shear Alfvén wave propagating along the interface has frequency kc_A. Thus, the cr ion for stability is that the growth rate in the absence of the field is less than the Alfvén wave frequency.

In the preceding analysis we forced the plasma to be incompressible by imposing Eqs. (9) and (10). If the plasma is allowed to be compressible, that is if we no longer assume that Eqs. (9) and (10) apply, we need an energy equation to close the system of MHD equations. A relatively simple energy equation is obtained by assuming that the plasma is adiabatic. In this case the specific entropy of the plasma p/ρ^Γ is a constant of the fluid motion, where Γ is the ratio of specific heats, so that

$$\left(\frac{\partial}{\partial t} + \boldsymbol{v}\cdot\nabla\right)\frac{p}{\rho^\Gamma} = 0. \tag{31}$$

In a fully ionised plasma $\Gamma = 5/3$. In the next section we use the linearised forms of Eq. (31) and Eqs. (4-8) to derive a single vector equation describing the MHD stability of a plasma.

2.2 The linearised MHD equations

When gravity, resistivity and equilibrium flows are neglected, and equilibrium and perturbed quantities are denoted, as before, by subscripts 0 and 1 respectively, the MHD equations, including now Eq. (31), take the following linearised form:

$$\frac{\partial \rho_1}{\partial t} + \nabla\cdot(\rho_0\boldsymbol{v}_1) = 0, \tag{32}$$

$$\rho_0\frac{\partial \boldsymbol{v}_1}{\partial t} + \nabla p_1 = \boldsymbol{j}_1\times\boldsymbol{B}_0 + \boldsymbol{j}_0\times\boldsymbol{B}_1, \tag{33}$$

$$\frac{\partial \boldsymbol{B}_1}{\partial t} = \nabla\times(\boldsymbol{v}_1\times\boldsymbol{B}_0), \tag{34}$$

$$\frac{\partial p_1}{\partial t} + (\boldsymbol{v}_1\cdot\nabla)p_0 + \Gamma(\nabla\cdot\boldsymbol{v}_1) = 0. \tag{35}$$

To obtain the linearised momentum equation [Eq. (33)] it is necessary to assume equilibrium force balance,

$$\nabla p_0 = \boldsymbol{j}_0\times\boldsymbol{B}_0, \tag{36}$$

and to obtain the linearised energy equation [Eq. (35)], it is necessary to use the continuity equation [Eq. (32)]. When using this set of equations to determine the stability of a particular configuration, it is useful to consider the spatial vector displacement $\boldsymbol{\xi}$ of the plasma from equilibrium:

$$\boldsymbol{v}_1 \equiv \left(\frac{\partial}{\partial t} + \boldsymbol{v}\cdot\nabla\right)\boldsymbol{\xi} \simeq \frac{\partial \boldsymbol{\xi}}{\partial t}. \tag{37}$$

Using Eq. (37) to eliminate $\mathbf{v}_1$ from Eqs. (32), (34) and (35), we can then integrate these equations with respect to time, bearing in mind that equilibrium quantities are, by definition, time-independent:

$$\rho_1 = -\nabla\cdot(\rho_0\boldsymbol{\xi}), \tag{38}$$

$$\boldsymbol{B}_1 = \nabla \times (\boldsymbol{\xi} \times \boldsymbol{B}_0)\,, \tag{39}$$

$$p_1 = -\boldsymbol{\xi} \cdot \nabla p_0 - \Gamma p_0 \nabla \cdot \boldsymbol{\xi}. \tag{40}$$

Substituting the expression for p_1 given by Eq. (40) into Eq. (33), and using Ampère's law [Eq. (8)] to eliminate the current density, we obtain

$$\rho_0 \frac{\partial^2 \boldsymbol{\xi}}{\partial t^2} = \nabla \left(\boldsymbol{\xi} \cdot \nabla p_0 + \Gamma p_0 \nabla \cdot \boldsymbol{\xi}\right) + \frac{1}{\mu_0} (\nabla \times \boldsymbol{B}_1) \times \boldsymbol{B}_0 + \frac{1}{\mu_0} (\nabla \times \boldsymbol{B}_0) \times \boldsymbol{B}_1. \tag{41}$$

For perturbations varying in time as $e^{-i\omega t}$ the left hand side of Eq. (41) becomes $-\omega^2 \rho_0 \boldsymbol{\xi}$. Eliminating $\boldsymbol{B}_1$ using Eq. (39), we then obtain an equation containing only spatial derivatives, in which the sole dependent variables are the three components of the plasma displacement $\boldsymbol{\xi}$. In general, for any specified set of boundary conditions, physically acceptable solutions exist only for certain values of ω^2. Thus, the stability of the configuration is determined by the solution of an eigenvalue problem. Bernstein et al. (1958) showed that, in the absence of equilibrium flows, the eigenvalues ω^2 are always real; it follows that a sufficient condition for instability is that the lowest value of ω^2 is negative.

For a uniform equilibrium plasma $\nabla p_0 = 0$ and $\nabla \times \boldsymbol{B}_0 = \boldsymbol{0}$. In this case it can be seen that Eq. (41) reduces to

$$\rho_0 \frac{\partial^2 \boldsymbol{\xi}}{\partial t^2} = \Gamma p_0 \nabla (\nabla \cdot \boldsymbol{\xi}) + \frac{1}{\mu_0} (\nabla \times \boldsymbol{B}_1) \times \boldsymbol{B}_0. \tag{42}$$

We will use this form of the momentum equation in the next subsection.

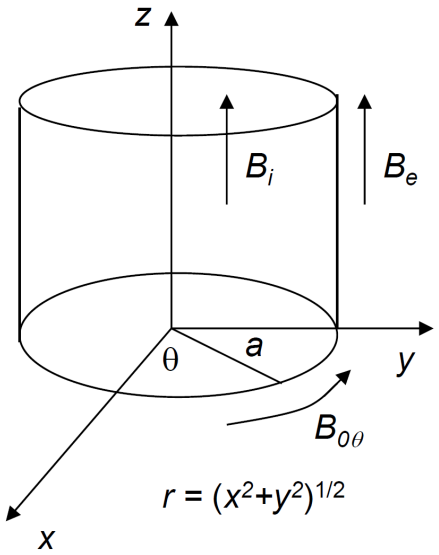

Fig. 3 Coordinate system and equilibrium magnetic fields used to analyse MHD stability of cylindrical plasma column.

2.3 Ideal MHD instabilities of a cylindrical plasma

Eq. (42) can be readily applied to the plasma column depicted in Fig. 3. In this figure we use right-handed cylindrical coordinates, (r, θ, z), and the column is assumed to be infinitely long, so that there are no boundaries in the axial (z) direction. In the equilibrium state, there are uniform axial magnetic fields B_i and B_e respectively inside and outside the plasma, which has radius a. An equilibrium current I is assumed to flow along the plasma boundary at $r = a$ in the z direction: Ampère's law then indicates that the azimuthal (θ) component of the equilibrium magnetic field is given by

$$\begin{aligned} B_{0\theta} &= 0, \qquad r < a, \\ &= \frac{\mu_0 I}{2\pi r}, \quad r > a. \end{aligned} \tag{43}$$

We consider plasma displacements of the form $\boldsymbol{\xi} = \boldsymbol{\xi}(r)\exp(ikz + im\theta - i\omega t)$, where periodicity requires m to be an integer. Cowling (1976) demonstrated that the change in potential energy δW associated with a perturbation $\boldsymbol{\xi}$ is minimised algebraically if the latter is divergence-free, i.e.

$$\nabla \cdot \boldsymbol{\xi} = \frac{1}{r}\frac{d}{dr}(r\xi_r) + \frac{im}{r}\xi_\theta + ik\xi_z = 0, \tag{44}$$

Since, as discussed at the beginning of this article, instability occurs if $\delta W < 0$, it follows that the most unstable ideal MHD modes are incompressible. The simple physical explanation for this is that less work is required to bend magnetic field lines if the plasma does not need to be compressed. We will therefore consider only incompressible perturbations of the cylindrical plasma column, and derive an expression for the ideal MHD eigenvalues of this system obtained originally by Kadomtsev (1966).

We consider first the plasma interior region ($r < a$) in which $B_{\theta 0} = 0$. Recalling the vector calculus identity $\nabla \times (\boldsymbol{a} \times \boldsymbol{b}) = \boldsymbol{a}(\nabla \cdot \boldsymbol{b}) - \boldsymbol{b}(\nabla \cdot \boldsymbol{a}) + (\boldsymbol{b} \cdot \nabla)\boldsymbol{a} - (\boldsymbol{a} \cdot \nabla)\boldsymbol{b}$, and also that k and B_i are the z-components of the perturbation wavevector and equilibrium magnetic field respectively, it follows from Eq. (44) and the linearised induction equation [Eq. (39)] that

$$\boldsymbol{B}_1 = ikB_i\boldsymbol{\xi}. \tag{45}$$

Since the equilibrium current density in the interior is $\boldsymbol{j}_0 = \nabla \times \boldsymbol{B}_0/\mu_0 = \boldsymbol{0}$, force balance requires that the equilibrium pressure is uniform, $\nabla p_0 = \boldsymbol{0}$. Since $\nabla \cdot \boldsymbol{\xi} = 0$ in the incompressible case we are considering, Eq. (40) then implies that $p_1 = 0$. Taking the divergence of Eq. (42), and using the results just derived, we obtain

$$\boldsymbol{B}_0 \cdot \nabla^2 \boldsymbol{\xi} = 0, \tag{46}$$

i.e.

$$\nabla^2 \xi_z = 0. \tag{47}$$

To progress from Eq. (47), we require the formula for the Laplacian operator in cylindrical coordinates:

$$\nabla^2 f = \frac{1}{r}\frac{\partial}{\partial r}\left(r\frac{\partial f}{\partial r}\right) + \frac{1}{r^2}\frac{\partial^2 f}{\partial \theta^2} + \frac{\partial^2 f}{\partial z^2}. \tag{48}$$

Given the assumed dependence of the displacement $\boldsymbol{\xi}$ on z and θ, it then follows that Eq. (47) can be written as the ordinary differential equation

$$\frac{d^2\xi_z}{dr^2} + \frac{1}{r}\frac{d\xi_z}{dr} - \left(k^2 + \frac{m^2}{r^2}\right)\xi_z = 0. \tag{49}$$

With the simple change of variable $u = kr$, Eq. (49) becomes

$$\frac{d^2\xi_z}{du^2} + \frac{1}{u}\frac{d\xi_z}{du} - \left(1 + \frac{m^2}{u^2}\right)\xi_z = 0, \tag{50}$$

which can be identified as the modified form of Bessel's equation (see e.g. Abramowitz and Stegun 1965). The solutions of this equation are modified Bessel functions of the first and second kind $I_m(u)$ and $K_m(u)$, which tend to infinity in the limits $u \to \infty$ and $u \to 0$, respectively. Since we are considering here the interior region, including $r = 0$, the required solutions in this region are proportional to $I_m(u) = I_m(kr)$. It is convenient to write

$$\xi_z(r) = \xi_z(a)\frac{I_m(kr)}{I_m(ka)}. \tag{51}$$

Writing down the components of Eq. (42) in cylindrical coordinates, using the appropriate form of the curl operator, neglecting the $\nabla \cdot \boldsymbol{\xi}$ term (since we are assuming incompressibility), and replacing $\mathbf{B}_1$ with $\boldsymbol{\xi}$ using Eq. (45), we find that the radial component of Eq. (42) can be rearranged to yield the following expression for ξ_r:

$$\xi_r(r) = \frac{ikB_i^2/\mu_0}{\omega^2\rho_0 - k^2B_i^2/\mu_0}\frac{d\xi_z}{dr}. \tag{52}$$

This can be evaluated using the solution obtained for ξ_z, i.e. Eq. (51).

We now turn to the exterior region. Outside the plasma there are no currents, so $\nabla \times \boldsymbol{B}_1 = 0$ and hence there exists a scalar function ψ such that $\boldsymbol{B}_1 = -\nabla\psi$. Moreover $\nabla \cdot \boldsymbol{B}_1 = 0$, so it follows that ψ, like ξ_z, must satisfy Laplace's equation, $\nabla^2\psi = 0$, which again takes the form given by Eq. (49). This time the required solutions are proportional to the functions $K_m(kr)$, which are nonsingular as $r \to \infty$:

$$\psi = C\frac{K_m(kr)}{K_m(ka)}\exp(ikz + im\theta - i\omega t). \tag{53}$$

Here, C is a constant to be determined by boundary conditions at the plasma edge.

Our choice of boundary conditions is motivated by the fact that when gravity is neglected the momentum equation [Eq. (5)] can be written in the form

$$\rho\left[\frac{\partial \boldsymbol{v}}{\partial t} + (\boldsymbol{v}\cdot\nabla)\boldsymbol{v}\right] = -\nabla\left(p + \frac{B^2}{2\mu_0}\right) + \frac{(\boldsymbol{B}\cdot\nabla)\boldsymbol{B}}{\mu_0}. \tag{54}$$

The final term on the right hand side of Eq. (54) is zero if the magnetic field lines are straight, so this term can be identified as a force arising from the magnetic tension associated with field line bending. This tension force is finite throughout the plasma

domain, and it follows from Eq. (54) that the total pressure (plasma plus magnetic) must be continuous across the boundary, since otherwise the gradient operator would produce an infinite force. Since $p_1 = 0$ in both the interior and exterior regions, the leading order perturbations to the magnetic pressure on the two sides of the boundary must be equal. We now proceed to evaluate these perturbations.

Inside the boundary, the perturbation to the magnetic pressure $B^2/2\mu_0$ is

$$\delta p_M^i = \frac{1}{2\mu_0}\delta\left(\boldsymbol{B}_0 + \boldsymbol{B}_1\right)^2 \simeq \frac{B_i B_{1z}}{\mu_0} = \frac{ikB_i^2}{\mu_0}\xi_z(a). \tag{55}$$

Here we have neglected the B_1^2 term and used Eq. (45). Outside the boundary, we have

$$2\mu_0\delta p_M^e \equiv \delta\left(\boldsymbol{B}_0 + \boldsymbol{B}_1\right)^2 \simeq \delta B_{0\theta}^2 + 2\left(B_e B_{1z} + B_{0\theta}B_{1\theta}\right), \tag{56}$$

where the first term on the right hand side arises from the fact that $B_{0\theta}$ depends on r, and the precise location of the boundary has changed due to the finite radial component of the plasma displacement $\boldsymbol{\xi}$. However ξ_z in Eq. (51) can be evaluated at $r = a$ rather than $r = a + \xi_r$ since ξ_z is itself a small quantity. To leading order,

$$B_{0\theta}^2(a + \xi_r) \simeq B_{0\theta}^2(a) + \xi_r \frac{\partial B_{0\theta}^2}{\partial r}|_{r=a}; \tag{57}$$

hence

$$\delta B_{0\theta}^2 \simeq \xi_r \frac{\partial B_{0\theta}^2}{\partial r}|_{r=a} = -\frac{2\xi_r(a)B_{0\theta}^2(a)}{a}, \tag{58}$$

where we have used Eq. (43) in the final step. The components of $\boldsymbol{B}_1 = -\nabla\psi$ can be evaluated using Eq. (53), and we deduce from Eq. (56) that the perturbation to the magnetic pressure outside the boundary is

$$\delta p_M^e = -\frac{\xi_r(a)B_{0\theta}^2(a)}{\mu_0 a} - \frac{C}{\mu_0}\left[ikB_e + \frac{im}{a}B_{0\theta}(a)\right]. \tag{59}$$

We may now set $\delta p_M^i = \delta p_M^e$, but to determine the constant C we require a further boundary condition, which is that the normal component of $\boldsymbol{B}$ be continuous. This is a standard corollary of the fact that $\nabla \cdot \boldsymbol{B} = 0$. In the perturbed state the normal direction at the boundary is not purely radial, since the plasma displacement depends on θ and z. When the radial distortion of the boundary is small, geometrical considerations lead us to conclude that the normal component of the magnetic field is given approximately by

$$B_n = \boldsymbol{B} \cdot \boldsymbol{n} \simeq B_{1r} - B_i \frac{\partial \xi_r}{\partial z} = B_{1r} - ikB_i\xi_r, \tag{60}$$

where $\boldsymbol{n}$ is the unit normal vector to the boundary. From Eq. (45) we see that the two terms on the right hand side cancel, giving $B_n = 0$. Hence the normal component of the magnetic field outside the boundary, which is given approximately by the expression

$$B_n \simeq B_{1r} - B_e\frac{\partial \xi_r}{\partial z} - \frac{B_{0\theta}}{a}\frac{\partial \xi_r}{\partial \theta} = B_{1r} - ik\xi_r B_e - \frac{im\xi_r}{a}B_{0\theta}, \tag{61}$$

must also vanish. Since $\boldsymbol{B}_1 = -\nabla\psi$, it follows from Eq. (53) that

$$B_{1r} = -\frac{\partial\psi}{\partial r} = -Ck\frac{K'_m(kr)}{K_m(ka)}e^{i(kz+m\theta-i\omega t)}. \tag{62}$$

Using Eqs. (61) and (62) to express C in terms of ξ_r, Eqs. (51) and (52) to relate $\xi_z(a)$ to $\xi_r(a)$, and setting $\delta p_M^i = \delta p_M^e$ using Eqs. (55) and (59), we finally obtain an equation in which $\xi_r(a)$ appears as a common factor. Cancellation of this factor yields the dispersion relation

$$\frac{\omega^2}{k^2} = \frac{B_i^2}{\mu_0\rho_0} - \frac{[kB_e + mB_{0\theta}(a)/a]^2}{\mu_0\rho_0 k^2}\frac{I'_m(ka)K_m(ka)}{I_m(ka)K'_m(ka)} - \frac{B_{0\theta}^2(a)}{\mu_0\rho_0 ka}\frac{I'_m(ka)}{I_m(ka)}. \tag{63}$$

We first note from this result that ω^2 is real, indicating that perturbations are either purely oscillatory ($\omega^2 > 0$) or purely growing ($\omega^2 < 0$). A second observation is that the modified Bessel functions of the first kind I_m are all monotonic increasing functions of their arguments, whereas the K_m are monotonic decreasing functions, and both I_m and K_m are always positive, so that the second term on the right hand side of Eq. (63) is invariably stabilising. The final term on the right hand side, on the other hand, is always negative and therefore destabilising.

We consider first the case of zero axial field in the external region ($B_e = 0$) and $m = 0$, i.e. an azimuthally symmetric perturbation. In the equilibrium state, the total internal pressure $p + B_i^2/2\mu_0$ is balanced by the external azimuthal magnetic field pressure $B_{0\theta}^2/2\mu_0$. The stability of this equilibrium is determined by Eq. (63), which reduces to

$$\frac{\omega^2}{k^2} = \frac{B_i^2}{\mu_0\rho_0} - \frac{B_{0\theta}^2(a)}{\mu_0\rho_0 ka}\frac{I'_0(ka)}{I_0(ka)}. \tag{64}$$

The function $I_0(x)$ has the property that $I'_0(x) < xI_0(x)/2$ for all x, therefore it follows from Eq. (64) that the system is stable for all wavenumbers k if

$$B_i^2 > B_{0\theta}^2(a)/2. \tag{65}$$

Conversely, an azimuthally symmetric *sausage* instability occurs if the external azimuthal field is sufficiently large compared to the internal axial field. The sausage instability, which occurs in Z-pinch experiments (Vikhrev et al. 1993), and possibly also in solar coronal loops (Pascoe et al. 2007), has a simple physical explanation. The boundary current I is constant, so a constriction of the plasma causes an increase in the external azimuthal field, since this scales as $1/r$, and hence the external pressure on the plasma is amplified. However further constriction of the plasma may be suppressed if there is an internal axial field B_i, because compression of magnetic flux in the plasma leads to an increase in the internal pressure, which opposes the increase in external pressure.

When perturbations with $m = 1$ grow in time, a *kink* instability is said to occur. Like the sausage instability, this is triggered if the azimuthal field is large enough compared to the internal axial field: an enhancement in B_θ again causes the external pressure on the plasma column to increase, thereby amplifying the perturbation in

the absence of any compensating stabilising effect. This can again be provided by the longitudinal field, but in this case there is no increase in the internal magnetic pressure, since the entire plasma column undergoes the same displacement at a given z, and so there is no compression of magnetic flux. Stabilisation in this case arises rather from the fact that the field lines inside the plasma are bent by the perturbation, producing the tension force which is represented by the last term on the right hand side of Eq. (54). This opposes the increase in external pressure.

To obtain a quantitative condition for the excitation of the kink instability we return to Eq. (63) and take the long wavelength limit $ka \ll 1$. In this limit $I_m \simeq (ka/2)^m/m!$ and $K_m \simeq (ka/2)^{-m}(m-1)!/2$ (when $m \neq 0$) (Abramowitz and Stegun 1965), so that Eq. (63) reduces to

$$\omega^2 = \frac{1}{\mu_0 \rho_0}\left[k^2 B_i^2 + (kB_e + mB_{0\theta}(a)/a)^2 - mB_{0\theta}^2(a)/a^2\right]. \tag{66}$$

We now consider the case in which both the internal and external longitudinal fields are large compared to the azimuthal field, i.e. $|B_i|, |B_e| \gg B_{0\theta}$, and the plasma beta $\beta = 2\mu_0 p/B_i^2 \ll 1$. This ordering applies in conventional tokamaks, although it should be noted that we are neglecting toroidal curvature effects since the equilibrium state considered here is a straight cylinder. Setting $B_i = B_e$, which is required by equilibrium pressure balance in this limit, and $m = 1$ in Eq. (66) we find that it reduces further to

$$\omega^2 = \frac{2k^2 B_e^2}{\mu_0 \rho_0}\left[1 + \frac{1}{ka}\frac{B_{0\theta}}{B_e}\right], \tag{67}$$

Since kB_e and $B_{0\theta}$ can have opposite sign, instability ($\omega^2 < 0$) can occur if

$$|B_\theta/B_e| > |ka|. \tag{68}$$

If there is no restriction on the values of k, an assumption which requires the plasma column to have infinite length, Eq. (68) indicates that the $m = 1$ mode is guaranteed to be unstable at sufficiently long wavelengths. If, on the other hand, the plasma has length L, it follows from Eq. (68) that instability will only occur if

$$|B_{0\theta}/B_e| > 2\pi a/L. \tag{69}$$

This result, known as the Kruskal-Shafranov condition (Kruskal 1954, Shafranov 1957), indicates that a kink instability occurs if the magnetic field on the surface is twisted by more than a complete circle about the cylinder axis from one end of the plasma to the other. For this reason it is sometimes referred to as the screw instability. The kink mode plays a key role in the stability of magnetically-confined fusion plasmas; it has also been proposed by Hood and Priest (1979) as a possible trigger of energy release in solar flares, and it may be important in other astrophysical plasmas. For example Li (2000) has pointed out that the Kruskal-Shafranov condition imposes constraints on the equilibrium magnetic field configurations that are possible in the vicinity of rotating black holes, thereby limiting the extent to which such objects can power extragalactic jets.

If the plasma column is bent round to form a torus of radius R, we have $L = 2\pi R$. The instability condition given by Eq. (69) can then be expressed in terms of the plasma safety factor q, which is defined in general as the number of toroidal circuits made by a field line for each poloidal circuit. In the large aspect ratio limit $R/a \gg 1$, the instability condition becomes

$$q = \frac{aB_e}{RB_{0\theta}(a)} < 1. \tag{70}$$

This simple result explains why burning plasma tokamaks need to have large toroidal magnetic fields. Plasmas in early magnetic confinement experiments were often grossly kink unstable because they did not have such fields (see e.g. Carruthers and Davenport 1957). The poloidal field $B_{0\theta}$ is proportional to the current I, which determines the pressure p of the plasma that can be confined by it via force balance (Bennett 1934), and p must be large enough for thermonuclear fusion reactions to occur at a sufficiently high rate. For the required value of the plasma current, Eq. (70) then gives the minimum toroidal field B_e needed to avoid the kink instability. The importance of doing so can be illustrated by estimating its growth rate if Eq. (70) were to be satisfied in a tokamak such as the burning plasma ITER device currently under construction. Assuming $B_e = B_{0\theta}$ and considering kink perturbations with $k = 1/R$, Eq. (66) yields the approximate growth rate

$$\gamma \simeq \frac{\sqrt{2}(R/a - 1)^{1/2}}{R} \frac{B_{0\theta}}{\sqrt{\mu_0 \rho}}. \tag{71}$$

Deuterium-tritium plasmas in ITER will have major and minor radii $R \simeq 6\,\mathrm{m}$ and $a \simeq 2\,\mathrm{m}$, particle densities $n \simeq 10^{20}\,\mathrm{m}^{-3}$, and poloidal magnetic fields $B_{0\theta} \sim 1\,\mathrm{T}$. Evaluating a growth time from Eq. (71) using these parameters, we obtain $1/\gamma \simeq 2 \times 10^{-6}\,\mathrm{s}$, which is about six orders of magnitude less than the required energy confinement time. ITER has been designed with $B_e \simeq 5\,\mathrm{T}$, giving $q > 1$ according to Eq. (70). Internal kink instabilities similar to those considered here may in fact occur in ITER, although with different physical drives (Chapman et al. 2011).

2.4 Ballooning modes

In the next two sub-sections we continue with the theme of MHD instabilities in toroidal plasmas, and briefly consider two important classes of instability which can limit the performance of tokamaks. In these devices the magnetic field lines, which are primarily toroidal, are concave towards the centre of the plasma on the outer side of the torus, and concave away from the plasma on the inner side, while the plasma pressure normally increases from the edge to the centre. This means that the field line curvature is unfavourable for ideal MHD stability on the outer side and favourable on the inner side (see e.g. Wesson 2004). An ideal MHD instability resulting from this effect is referred to as a *ballooning mode*. Using the fact that the radius of curvature of the magnetic field lines is of the order of the tokamak major radius R, one can show that the destabilising contribution per unit volume of a radial pressure gradient dp/dr to

the potential energy associated with a radial plasma displacement ξ on the outer side of a tokamak plasma is given approximately by

$$\delta W_p \sim -\frac{1}{R}\frac{dp}{dr}\xi^2. \tag{72}$$

Now the energy density required to bend the field lines δW_B can be estimated from the linearised, time-integrated form of the induction equation [Eq. (39)]:

$$\delta W_B = \frac{B_1^2}{2\mu_0} \sim k_\parallel^2 \xi^2 \frac{B_0^2}{2\mu_0}, \tag{73}$$

where $k_\parallel$ is the wavenumber associated with the variation of ξ along the field. Given that ξ is expected to be finite in the unfavourable curvature region, and close to zero in the favourable curvature region, it follows from the definition of q that $k_\parallel \sim 1/qR$. Instability will occur if the destabilising energy exceeds that required to bend the field lines, i.e. $\delta W_p > \delta W_B$; it follows from Eqs. (72) and (73) that ballooning instability may be expected if

$$-\frac{dp}{dr} > \frac{B_0^2}{\mu_0 q^2 R}. \tag{74}$$

A more quantitative analysis by Connor et al. (1978) shows that the stability of this type of mode also depends on the local magnetic shear, $s = d\ln q/d\ln r$.

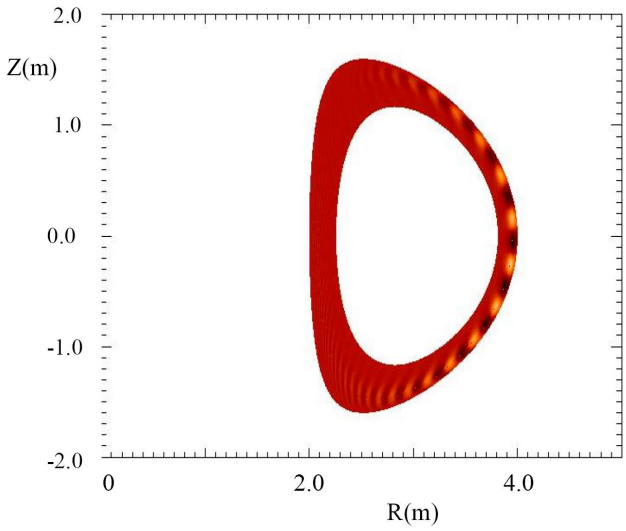

Fig. 4 Structure in the poloidal plane of a peeling-ballooning mode in a JET-like tokamak plasma, computed using the ELITE code (Snyder et al. 2002). It can be seen that the mode amplitude peaks on the outer ("bad curvature") side of the torus.

Ballooning modes limits the pressure and hence the fusion performance that can be achieved in tokamak plasmas. In particular, when coupled to *peeling modes* (edge-localised perturbations that become unstable when the local current density gradient becomes sufficiently large), they are believed to play an important role in controlling the stability of a density and temperature pedestal region close to the plasma edge in high confinement (*H-mode*) discharges (Snyder et al. 2002). Figure 4 shows the structure in the poloidal (R, Z) plane of a peeling-ballooning mode calculated for a plasma with parameters similar to those in the Joint European Torus (JET). Ballooning instabilities in H-mode plasmas are linked to the triggering of *edge localised modes* (ELMs), which are periodic bursts of light emission associated with particle and heat loss from the plasma. ELMs involve the formation of localised filaments, with density and temperature characteristic of the H-mode pedestal, that eventually detach from the plasma. This is a critical issue for ITER, since ELMs in that device will need to be mitigated or suppressed if unacceptable damage to plasma-facing components is to be avoided (Schaffer et al. 2008).

2.5 Tearing modes

Plasma configurations with finite resistivity η can be unstable even when they are stable in the ideal limit ($\eta \to 0$), the physical reason for this being that the magnetic field has more degrees of freedom when it is not frozen into the fluid. A *tearing instability* in a toroidal plasma with finite resistivity is driven by a radial gradient of the equilibrium toroidal current density j_φ. The temperatures and densities in tokamak plasmas are such that the resistivity is very low, in the sense that the evolution of magnetic field perturbations is governed to a very good approximation across most of the plasma by

the ideal MHD form of the induction equation [Eq. (28)], and the inertia term in the momentum equation can also usually be neglected in this region, so that force balance is described by

$$\nabla p = \boldsymbol{j} \times \mathbf{B}. \tag{75}$$

Applying the curl operator to Eq. (75) yields

$$\nabla \times (\boldsymbol{j} \times \mathbf{B}) = 0, \tag{76}$$

We apply this equation to a large aspect ratio toroidal plasma, denoting as before minor radial distance by r, poloidal angle by θ, and introducing a *helical flux* ψ such that the perturbation to the otherwise axisymmetric magnetic field has components

$$B_{1r} = -\frac{1}{r}\frac{\partial \psi}{\partial \theta}, \qquad B_{1\theta} = \frac{\partial \psi}{\partial r}. \tag{77}$$

Denoting toroidal angle by φ, periodicity in this coordinate and in θ requires perturbations to vary as $\exp(im\theta - in\varphi)$ where m and n are integers. Linearising Eq. (76) for perturbations of this form, and taking the large aspect ratio limit ($R/a \gg 1$), it can be shown (Wesson 2004) that the toroidal component of this equation reduces to

$$\frac{1}{r}\frac{d}{dr}\left(r\frac{d\psi}{dr}\right) - \frac{m^2}{r^2}\psi - \frac{\mu_0 dj_\varphi/dr}{B_\theta(1 - nq/m)} = 0, \tag{78}$$

where j_φ and B_θ denote respectively the toroidal component of the equilibrium current density and the poloidal component of the equilibrium magnetic field, while q as before is the safety factor, evaluated here using the local values of r and B_θ. It is immediately apparent that Eq. (78) has a singularity at the resonant surface $r \equiv r_s$ where $q = m/n$; there is a discontinuity Δ' in $(d\psi/dr)/\psi \equiv \psi'/\psi$ at this surface, which plays a crucial role in tearing mode theory (Wesson 2004).

In a thin layer around $r = r_s$ neither inertia nor resistivity can be neglected, and Eq. (78) does not apply. Instead we have to use the linearised forms of the full momentum and induction equations; the former is given by Eq. (27), with the gravitational force term neglected, while in the case of uniform η the latter is given by

$$\frac{\partial \boldsymbol{B}_1}{\partial t} = \nabla \times (\boldsymbol{v}_1 \times \boldsymbol{B}_0) + \frac{\eta}{\mu_0}\nabla^2 \boldsymbol{B}_1. \tag{79}$$

For perturbations varying as $\exp(\gamma t + im\theta - in\varphi)$, it can be shown (Wesson 2004) that the radial components of these equations yield the dispersion relation

$$\Delta' = 2.12\mu_0 \gamma d/\eta, \tag{80}$$

where d, a characteristic radial width of the resistive layer, is given by

$$d = \left(\frac{\rho\eta\gamma r^2 q^2}{B_\theta^2 m^2 q'^2}\right)^{1/4}. \tag{81}$$

Here, $q' = dq/dr$. Noting that d itself depends on the growth rate γ, we can use Eqs. (80) and (81) to derive an expression for this quantity:

$$\gamma = \frac{0.55}{\tau_R^{3/5}\tau_A^{2/5}}\left(n\frac{a}{R}\frac{aq'}{q}\right)^{2/5}(a\Delta')^{4/5}, \tag{82}$$

where $\tau_A = a(\mu_0\rho)^{1/2}/B_\varphi$ is an Alfvén time and $\tau_R = \mu_0 a^2/\eta$ is a resistive diffusion time. If we take the plasma minor radius a to be a characteristic macroscopic lengthscale, τ_A can be identified as the timescale associated with the $\boldsymbol{j}_1 \times \boldsymbol{B_0}$ term in the linearised momentum equation [Eq. (27)] and the $\nabla \times (\boldsymbol{v}_1 \times \boldsymbol{B}_0)$ term in the linearised induction equation [Eq. (79)], while it can be seen from Eq. (79) that τ_R is the timescale associated with the resistive term in that equation if we again take a to be the relevant lengthscale. To obtain Eq. (82) it is necessary to use the fact that $q \simeq (r/R)B_\varphi/B_\theta$ for a large aspect ratio toroidal plasma, and at the resonant surface $q = m/n$. It follows from this result that instability occurs if $\Delta' > 0$, but the calculation of this quantity is not straightforward. The factors other than τ_A and τ_R in Eq. (82) typically combine to give an overall dimensionless factor of order unity, which means that the tearing mode growth time is intermediate between the Alfvénic timescale and the much longer resistive timescale (it should be noted that the latter would be much shorter if it were calculated using d rather than a).

In hot tokamak plasmas the value of d given by Eq. (81) can be smaller than the ion Larmor radius, in which case the MHD model of the resistive layer used to derive the above results is not self-consistent, and kinetic effects need to be taken into account.

3 Two-fluid and kinetic instabilities

In the remainder of this article we will discuss plasma instabilities which can only be understood by treating the electron and ion populations as separate entities. Despite the fact that temperatures much higher than those normally occurring on Earth are required for matter to be fully ionised, it is permissible to treat the electrons and ions in a plasma as cold fluids provided that their dynamical behaviour is determined primarily by forces other than the pressure gradient force. The presence of any electric field $\boldsymbol{E}$ in the plasma produces forces in the electron and ion fluid momentum equations, which have no analogue in the MHD momentum equation [Eq. (4)]. In certain circumstances, these electric field forces give rise to the two-stream instability discussed below. This is an example of a cold plasma instability. If finite temperature effects are important, it may still be possible to use a two-fluid (or multi-fluid) model provided that a suitable closure scheme for the equations can be found. However in many circumstances no practical fluid closure scheme exists, and it is then appropriate to use a kinetic approach to stability analysis.

3.1 Two-stream (Buneman) instability

This belongs to a class of instabilities referred to as *electrostatic*, meaning that only the electric field is perturbed.[2] Consider an electrically-neutral uniform equilibrium plasma with electrons streaming at velocity v_0 along the magnetic field (x) direction relative to singly-charged ions, which are taken to be at rest in the equilibrium state. This is actually a very common scenario, since by definition there must be a net flow of electrons with respect to ions in any current-carrying plasma. We assume that the plasma is "cold" in the sense that v_0 is large compared to the electron and ion thermal speeds, and that any spatial variations occur only in the x-direction. Thus, Poisson's equation

$$\nabla \cdot \boldsymbol{E} = \frac{\rho_c}{\epsilon_0}, \tag{83}$$

where ρ_c is charge density and ϵ_0 is free space permittivity, takes the form

$$\frac{\partial E_1}{\partial x} = \frac{e(n_{i1} - n_{e1})}{\epsilon_0}. \tag{84}$$

Here, n_{1i}, n_{1e} are the perturbations to the common ion and electron equilibrium number density n_0 and $-e$ is the electron charge. In general the momentum equations of cold ion and electron fluids can be written in the form

$$m_i n_i \left[\frac{\partial \boldsymbol{v}_i}{\partial t} + (\boldsymbol{v}_i \cdot \nabla)\boldsymbol{v}_i\right] = e n_i \boldsymbol{E} + e n_i \boldsymbol{v}_i \times \boldsymbol{B}, \tag{85}$$

$$m_e n_e \left[\frac{\partial \boldsymbol{v}_e}{\partial t} + (\boldsymbol{v}_e \cdot \nabla)\boldsymbol{v}_e\right] = -e n_e \boldsymbol{E} - e n_e \boldsymbol{v}_e \times \boldsymbol{B}, \tag{86}$$

where m_i, m_e denote the ion and electron masses, $n_i = n_0 + n_{i1}$ and $n_e = n_0 + n_{e1}$ are the total ion and electron number densities and $\boldsymbol{v}_i$, $\boldsymbol{v}_e$ are the ion and electron fluid velocities. In the ion rest frame there is, by definition, no equilibrium ion flow, and so the x-component of Eq. (85) has the linearised form

$$m_i n_0 \frac{\partial v_{i1}}{\partial t} = e n_0 E_1, \tag{87}$$

where v_{i1} is the perturbation to $\boldsymbol{v}_i$ in the x-direction. The linearised x-component of Eq. (86) is similar to Eq. (87), but there is an additional term on the left hand side arising from the equilibrium flow v_0:

$$m_e n_0 \left(\frac{\partial v_{e1}}{\partial t} + v_0 \frac{\partial v_{e1}}{\partial x}\right) = -e n_0 E_1, \tag{88}$$

where m_e is the electron mass and v_{e1} is the perturbation to $\boldsymbol{v}_e$ in the x-direction. To close the system of equations we require also the continuity equations for the two species, which have the general form

$$\frac{\partial n_i}{\partial t} + \nabla \cdot (n_i \boldsymbol{v}_i) = 0, \tag{89}$$

[2]This is of course a misnomer, since in such cases the perturbed electric field is clearly not static.

$$\frac{\partial n_e}{\partial t} + \nabla \cdot (n_e \boldsymbol{v}_e) = 0. \tag{90}$$

It is straightforward to establish that Eq. (89) has the linearised form

$$\frac{\partial n_{i1}}{\partial t} + n_0 \frac{\partial v_{i1}}{\partial x} = 0. \tag{91}$$

while Eq. (90) has the linearised form

$$\frac{\partial n_{e1}}{\partial t} + n_0 \frac{\partial v_{e1}}{\partial x} + v_0 \frac{\partial n_{e1}}{\partial x} = 0. \tag{92}$$

For propagating wave solutions of the form $\exp(ikx - i\omega t)$, Eqs. (84), (87), (88), (91) and (92) yield the set of algebraic equations

$$ikE_1 = \frac{e}{\epsilon_0}(n_{i1} - n_{e1}), \tag{93}$$

$$-i\omega m_i n_0 v_{i1} = e n_0 E_1, \tag{94}$$

$$-im_e n_0(\omega - kv_0)v_{e1} = -e n_0 E_1, \tag{95}$$

$$-i\omega n_{i1} + ikn_0 v_{i1} = 0, \tag{96}$$

$$-in_{e1}(\omega - kv_0) + ikn_0 v_{e1} = 0. \tag{97}$$

Using the continuity equations [Eqs. (96) and (97)] to express the density perturbations in terms of the velocity perturbations, eliminating the latter using the momentum equations [Eqs. (94) and (95)], and finally substituting the resulting expressions for n_{i1} and n_{e1} into Poisson's equation [Eq. (93)], we obtain the following dispersion relation, first derived by Buneman (1958):

$$1 - \frac{\omega_{pi}^2}{\omega^2} - \frac{\omega_{pe}^2}{(\omega - kv_0)^2} = 0, \tag{98}$$

where $\omega_{pi} = (n_0 e^2/m_i\epsilon_0)^{1/2}$, $\omega_{pe} = (n_0 e^2/m_e\epsilon_0)^{1/2}$ are the ion and electron plasma frequencies. The quantity kv_0 in the denominator of the last term on the left hand side can be regarded as a Doppler shift: if we had considered the problem in the rest frame of the electrons instead of the ions, this term would have appeared as ω_{pe}^2/ω^2. It is evident that Eq. (98) can be rewritten as a fourth order polynomial equation for ω, indicating that four roots must exist. Moreover the coefficients of each power of ω in this polynomial equation are all real, indicating that any complex roots must occur in conjugate pairs, i.e. they are of the form $\omega = \omega_0 \pm i\gamma$ where ω_0, γ are real. One of these is growing exponentially in time, and therefore the existence of any non-real roots implies instability.

To determine the conditions for instability, it is useful to consider the function

$$F(\omega) = \frac{\omega_{pi}^2}{\omega^2} + \frac{\omega_{pe}^2}{(\omega - kv_0)^2}. \tag{99}$$

Roots of the two-stream dispersion relation then correspond to $F = 1$. It is easier to visualise the shape of $F(\omega)$ if artificially low values are assigned to $(\omega_{pe}/\omega_{pi})^2 = m_i/m_e$.

Setting the mass ratio equal to 100, and plotting F as a function of ω/ω_{pe} (treated as a real number) for two specified values of kv_0/ω_{pe}, we obtain the curves shown in Fig. 5. In the left hand plot the curve intersects $F = 1$ four times. Since $F = 1$ is the condition for a root to exist, and we know that there are four roots of Eq. (98) in total, it follows that in this case the roots are all real and therefore there is no instability. In the right hand plot, on the other hand, the curve intersects $F = 1$ only twice, from which we infer that two of the four roots cannot be found by plotting F versus real values of ω. These roots must be complex, and therefore instability occurs at this wavenumber.

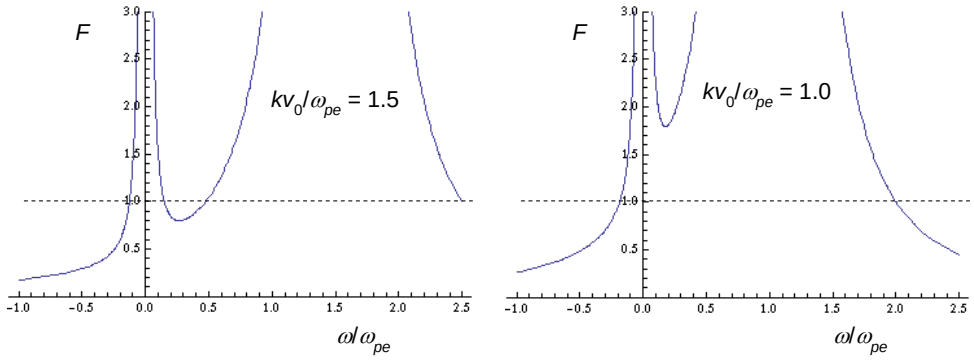

Fig. 5 The function F for $m_i/m_e = 100$ and two values of kv_0/ω_{pe}. Real frequency solutions of the two-stream dispersion relation correspond to $F = 1$, indicated by dashed lines.

From Fig. 5 it is clear that instability occurs when $F > 1$ for values of ω such that $dF/d\omega = 0$. Defining $\mu = m_e/m_i$ we find that $dF/d\omega = 0$ for

$$\omega = \frac{kv_0\mu^{1/3}}{1+\mu^{1/3}}. \tag{100}$$

Using this expression to eliminate ω from F we find that $F > 1$ if

$$kv_0 < (1+\mu^{1/3})^{3/2}\omega_{pe}, \tag{101}$$

indicating that, for any given electron/ion streaming velocity v_0, all modes in an infinite system with wavelengths above a certain value are unstable. In a plasma of finite length L, there is a minimum value of k given by $k_{\min} = 2\pi/L$. and no instability occurs if Eq. (101) is not satisfied for $k = k_{\min}$.

For $\mu = 1/1836$ (a hydrogen plasma), the mode frequency at the threshold wave number for instability is given by

$$\omega_0 = \mu^{1/3}(1+\mu^{1/3})^{1/2}\omega_{pe} \simeq 0.08\omega_{pe} \simeq 3.6\omega_{pi}. \tag{102}$$

Close to the threshold, the unstable mode frequencies thus lie between the electron and ion plasma frequencies, although closer to the latter. The natural oscillation frequency of the electron fluid is ω_{pe}, but due to the streaming velocity v_0 this can be Doppler-shifted in the ion rest frame to a frequency of the order of ω_{pi}, which is the natural

oscillation frequency of the ion fluid; a strong collisionless interaction of the two fluids is thus possible, and the streaming of the electrons with respect to the ions provides free energy to drive instability.

Rearranging Eq. (98) and assuming that $|\omega|^2 >> \omega_{pi}^2$, we obtain

$$\frac{kv_0}{\omega_{pe}} - \frac{\omega}{\omega_{pe}} = \left(1 - \frac{\omega_{pi}^2}{\omega^2}\right)^{-1/2} \simeq 1 + \frac{\omega_{pi}^2}{2\omega^2}. \tag{103}$$

Putting $\omega = |\omega| e^{i\theta}$ in this equation and equating imaginary terms, we obtain

$$|\omega| = \omega_{pi}^{2/3} \omega_{pe}^{1/3} \cos^{1/3}\theta, \tag{104}$$

and hence the growth rate

$$\gamma = |\omega| \sin\theta = \omega_{pi}^{2/3} \omega_{pe}^{1/3} \cos^{1/3}\theta \sin\theta. \tag{105}$$

The function of θ in this expression has a stationary value at $\theta = \pi/3$, and therefore the maximum growth rate of the two-stream instability is

$$\gamma_{\max} = (\sqrt{3}\mu^{1/3}/2^{4/3})\omega_{pe}. \tag{106}$$

In laboratory plasmas this can be extremely high. For a deuterium plasma in JET with particle density $n = 4 \times 10^{19}\,\mathrm{m}^{-3}$, for example, this expression yields a growth time $1/\gamma_{\max} \sim 10^{-10}\,\mathrm{s}$. However the two-stream instability does not in fact usually occur in tokamak plasmas, due to the process known as *Landau damping* [for a physically-transparent discussion of this phenomenon, see Wesson (2015)]. In the above analysis we assumed that the electron-ion drift speed v_0 was large compared to the electron and ion thermal speeds. In JET the toroidal plasma current density is typically of the order of $10^6\,\mathrm{Am}^{-2}$; this figure, combined with the particle density assumed above, implies an electron-ion drift speed of around $2 \times 10^5\,\mathrm{ms}^{-1}$, while the electron thermal speed in the plasma core is generally more than two orders of magnitude greater than this. The cold plasma model is therefore not applicable and kinetic effects associated with Landau damping suppress the two-stream instability. However, there are many other plasmas [for example high current discharge plasmas (Takeda and Yamagiwa 1985), the Earth's ionosphere (Oppenheim et al. 1996) and supernova remnants (McClements et al. 2001)] in which this instability can occur.

3.2 Bump-on-tail instability

In the remainder of this article we will consider purely kinetic instabilities in the collisionless limit. These are described in general by the Vlasov equation, combined self-consistently with Maxwell's equations. The bump-on-tail instability is the most straightforward to analyse since, like the two-stream instability, it is a purely electrostatic mode arising from charge separation between ions and electrons. In the simplest case the excited waves are driven at frequencies of order ω_{pe} by a relative streaming of one electron population (the "bump") with respect to another. These waves propagate

along a uniform equilibrium field $\boldsymbol{B}_0$, which we choose to be in the x-direction. The ions are regarded as infinitely massive and serve only to provide charge neutrality in the equilibrium state. A linearisation procedure can be used, as in fluid models, but one of the linearised quantities is now the one-dimensional electron distribution function $f(x, v, t)$ (where v is electron velocity in the x-direction), which we write as the sum of an equilibrium term f_0 and a perturbation f_1. The equilibrium electric field, as in the case of the two-stream instability, is taken to be zero, and both the perturbed electric field E_1 and f_1 are assumed to have the form of a wave propagating in the x-direction, i.e. E_1, $f_1 \propto \exp(ikx - i\omega t)$. The linearised form of the Vlasov equation is (Chen 1984)

$$\frac{\partial f_1}{\partial t} + v\frac{\partial f_1}{\partial x} - \frac{e}{m_e}E_1\frac{\partial f_0}{\partial v} = 0. \tag{107}$$

We also require Poisson's equation, which now takes the integro-differential form

$$\frac{\partial E_1}{\partial x} = -\frac{e}{\epsilon_0}\int_{-\infty}^{\infty} f_1 dv. \tag{108}$$

The equilibrium electron distribution f_0 does not appear in this equation since its integral over v is equal to the equilibrium electron density n_0, which cancels the ion density exactly if, as assumed, there is no equilibrium electric field. Equations (107) and (108) can be combined to give the relation (Chen 1984)

$$1 = \frac{\omega_{pe}^2}{k^2}\int_{-\infty}^{\infty} \frac{\partial F/\partial v}{v - \omega/k} dv, \tag{109}$$

where $F = f_0/n_0$. We consider first the case of a pure Maxwellian electron distribution of the form

$$F = \frac{1}{\sqrt{2\pi}v_{te}} \exp\left(-\frac{v^2}{2v_{te}^2}\right), \tag{110}$$

where $v_{te} = (T_e/m_e)^{1/2}$, T_e being the electron temperature. In the limit $\omega/k \gg v_{te}$, we can expand the denominator of the integrand in Eq. (109) in ascending powers of kv/ω, using the fact that the integrand is vanishingly small for $v \gg v_{te}$, yielding the leading order result

$$1 = \frac{\omega_{pe}^2}{\omega^2}. \tag{111}$$

Thus we recover $\omega = \omega_{pe}$, which describes electron plasma oscillations. However in general the solutions $\omega = \omega(k)$ of Eq. (109) are complex with a finite imaginary part γ whose sign, as usual, determines whether instability occurs. Evaluation of γ is not immediately straightforward since it moves the pole from the real velocity line to a point above or below it, corresponding respectively to instability or stability. If F is a pure Maxwellian, as in Eq. (110), the pole yields damping, $\gamma < 0$ (Chen 1984).

Here we assume *a priori* that there is a non-Maxwellian component in F that produces instability, and deduce a condition for that to be the case. We consider the semi-circular contour in the complex v plane shown in Fig. 6: the semi-circle has radius v_r which is larger than γ/k but small enough that $\partial F/\partial v$ does not vary significantly

over the region bounded by the contour. It follows from the residue theorem that the value of the integral around the closed (Jordan) contour is $2\pi i \partial F/\partial v$ where $\partial F/\partial v$ is evaluated at $v \simeq \omega_{pe}/k$. We can also evaluate the integral along the semi-circular part of the contour *alone* by making the substitution $v - \omega_{pe}/k = e^{i\theta}$ and integrating from $\theta = 0$ to π, using the assumption that $\partial F/\partial v$ can be treated as a constant along this semi-circle. It is straightforward to establish that this integral has the value $\pi i \partial F/\partial v$. However the integral we actually need is the one along the section of the contour that lies on the real v line, and this is simply the difference between the closed contour integral and the semi-circular contribution, that is to say $\pi i \partial F/\partial v$. Evaluating the real part of the integral in Eq. (109) using the same ordering as before ($\omega/k \gg v_{te}$), but including now the contribution of the pole, we obtain

$$1 = \frac{\omega_{pe}^2}{k^2}\left[\frac{k^2}{\omega^2} + i\pi\left(\frac{\partial F}{\partial v}\right)_{v=\omega_{pe}/k}\right]. \tag{112}$$

Using $\gamma \ll \omega_{pe}$, it is straightforward to infer from Eq. (112) that

$$\frac{\gamma}{\omega_{pe}} \simeq -\frac{\pi}{2}\frac{\omega_{pe}^2}{k^2}\left(\frac{\partial F}{\partial v}\right)_{v=\omega_{pe}/k}. \tag{113}$$

For a pure Maxwellian F this result yields Landau damping. It is however valid for distributions which are non-Maxwellian at the resonant velocity $v = \omega/k$ provided that the bulk of the distribution remains Maxwellian. Suppose, for example, the electron distribution is of the form shown in Fig. 6, with a dominant Maxwellian core centred on zero velocity and a dilute bump-on-tail at $v > v_{te}$, so that $\partial F/\partial v > 0$ for some range of suprathermal speeds. The principal part of the integral in Eq. (109) (that is to say, the value of integral when the singularity at $v = \omega/k$ is neglected) does not change significantly, provided that the bump-on-tail is sufficiently dilute, and therefore the real frequency is still given by Eq. (111). However Eq. (113) indicates that electron plasma oscillations with $\omega/k = \omega_{pe}/k = v$ such that $\partial F/\partial v > 0$ are unstable. This *bump-on-tail instability* can be regarded as a kinetic (finite-temperature) analogue of the two-stream instability.

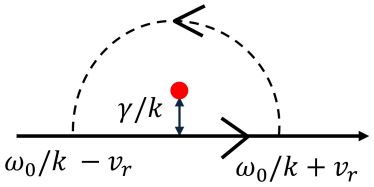

Fig. 6 Region of complex velocity space containing the pole (large red dot) that gives rise to the bump-on-tail instability. The arrows indicate the direction of the contour integration that must be performed to obtain the growth rate.

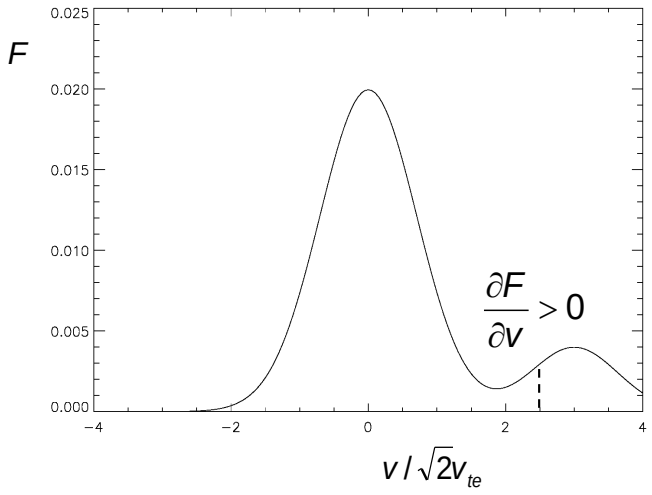

Fig. 7 Schematic plot of a one-dimensional bump-on-tail distribution. Waves with phase velocity indicated by the dashed line are unstable.

Both Landau damping and the bump-on-tail instability arise from a wave-particle resonance: the wave frequency is Doppler-shifted to zero in a frame moving along $\boldsymbol{B}_0$ at velocity $v = \omega_{pe}/k$. In this frame the wave electric field is static, and so a strong interaction can occur between the wave and any particles moving at that velocity. For any finite wave amplitude there is a range of velocities above and below the resonance in which particles are trapped by the wave. Oscillatory motion of particles within the trapped region causes the formation of a plateau in velocity space. Particles that were initially above the resonance lose energy, on average, and particles that were initially below the resonance gain energy. If $\partial F/\partial v > 0$ there are more of the former than of the latter, resulting in a net loss of particle kinetic energy. Since energy is conserved, and there is no exchange of energy with other particle species (we are considering a collisionless system), the wave is amplified.

The bump-on-tail instability is believed to cause *type III solar radio bursts* (see e.g. Robinson and Cairns 1998). In this case the bump is produced by fast electrons overtaking slow ones as they propagate away from the Sun. The initial instability produces electrostatic waves at frequencies close to the local electron plasma frequency; these are mode converted to electromagnetic waves at frequencies around ω_{pe} and $2\omega_{pe}$, subsequently being detected on Earth as radio emission. Because the electrons exciting the instability are propagating away from the Sun, and hence through a solar wind plasma of diminishing density, the emission is observed to chirp down in frequency during each burst. The same type of instability has also been invoked to explain electrostatic waves observed close to Earth's bow shock (Cairns and Robinson 1999) and magnetotail (Omura et al. 1996), and forms the basis of a simplified model proposed for Alfvénic instabilities excited by energetic ions in tokamaks (Berk and Breizman 1990).

It should be noted that Eqs. (112) and (113) are only valid in the limit $\omega/k \gg v_{te}$. When F is Maxwellian, the exact dispersion relation Eq. (109) can be written in the

form

$$\frac{2k^2v_{te}^2}{\omega_{pe}^2} = Z'\left(\frac{\omega}{\sqrt{2}kv_{te}}\right) = -2\left[1 + \frac{\omega}{\sqrt{2}kv_{te}}Z\left(\frac{\omega}{\sqrt{2}kv_{te}}\right)\right], \tag{114}$$

where

$$Z(\zeta) \equiv \frac{1}{\sqrt{\pi}}\int_{-\infty}^{\infty}\frac{e^{-t^2}dt}{t-\zeta} \quad [\mathrm{Im}(\zeta) > 0], \tag{115}$$

is referred to as the *plasma dispersion function* (Fried and Conte 1961). It is useful to cast the dispersion relation in the form given by Eq. (114) since the properties of the complex variable function Z, although somewhat complicated, are well-known and computer routines used to evaluate it are widely available. The electron distribution F can often be approximated by one or more Maxwellian components, possibly drifting with respect to each other or with unequal temperatures parallel and perpendicular to the magnetic field. The dispersion relation can then be formulated in terms of Z, and readily solved numerically. For example, a more exact analysis of the bump-on-tail instability can be performed by modelling the bump as a drifting Maxwellian and solving the exact dispersion relation numerically. McQuillan and McClements (1988) showed that the unstable mode is strongly modified if the bump is sufficiently dense or cold.

3.3 Electromagnetic instabilities

The two-stream and bump-on-tail instabilities do not depend on the equilibrium magnetic field $\boldsymbol{B}_0$ because the particle drifts, the wave electric field $\boldsymbol{E}_1$ and the wave vector $\boldsymbol{k}$ are all parallel to $\boldsymbol{B}_0$. In these circumstances it follows from Faraday's law that the magnetic field associated with a harmonic perturbation varying as $\exp(i\boldsymbol{k}\cdot\boldsymbol{x} - i\omega t)$ is identically zero:

$$i\omega\boldsymbol{B}_1 = i\boldsymbol{k}\times\boldsymbol{E}_1 = \boldsymbol{0}, \tag{116}$$

and therefore the instability is electrostatic. For electromagnetic waves ($\boldsymbol{B}_1$, $\boldsymbol{E}_1 \neq 0$) propagating in arbitrary directions with respect to a uniform equilibrium field $\boldsymbol{B}_0$, the linearised Vlasov equation for nonrelativistic electrons or ions of charge q, mass m is

$$\frac{\partial f_1}{\partial t} + \boldsymbol{v}\cdot\nabla f_1 + \frac{q}{m}(\boldsymbol{v}\times\boldsymbol{B}_0)\cdot\frac{\partial f_1}{\partial \boldsymbol{v}} = -\frac{q}{m}(\boldsymbol{E}_1 + \boldsymbol{v}\times\boldsymbol{B}_1)\cdot\frac{\partial f_0}{\partial \boldsymbol{v}}. \tag{117}$$

As before, the equilibrium electric field is assumed to be zero. The perturbed fields $\boldsymbol{E}_1$ and $\boldsymbol{B}_1$ are of course coupled through Maxwell's equations, and both depend on first moments of the perturbed distributions functions f_1, since these determine the plasma current (necessarily zero in the equilibrium state, since $\boldsymbol{B}_0$ is uniform).

Since the unperturbed distribution f_0 is uniform and time-independent, it must satisfy the equation

$$(\boldsymbol{v}\times\mathbf{B}_0)\cdot\frac{\partial f_0}{\partial \boldsymbol{v}} = 0. \tag{118}$$

We take $\boldsymbol{B}_0$ to lie in the z-direction and introduce velocity-space coordinates $v_\parallel$, $v_\perp$ and gyrophase angle α such that

$$v_x = v_\perp\cos\alpha, \qquad v_y = v_\perp\sin\alpha, \qquad v_z = v_\parallel. \tag{119}$$

Equation (118) indicates that $v_y \partial f_0/\partial v_x = v_x \partial f_0/\partial v_y$, from which it follows that

$$\frac{\partial f_0}{\partial \alpha} = \frac{\partial f_0}{\partial v_x}\frac{\partial v_x}{\partial \alpha} + \frac{\partial f_0}{\partial v_y}\frac{\partial v_y}{\partial \alpha} = 0, \tag{120}$$

so that $f_0 = f_0(v_\parallel, v_\perp)$. It is well-known that $v_\parallel$ and $v_\perp$ are conserved for a collisionless charged particle in a plasma with a uniform magnetic field and zero electric field, and so it may be inferred that f_0 can be expressed as a function of the particle constants of motion.

Equation (117) can be solved for f_1 by writing it in the form

$$\frac{Df_1}{Dt} = -\frac{q}{m}(\boldsymbol{E}_1 + \boldsymbol{v} \times \boldsymbol{B}_1) \cdot \frac{\partial f_0}{\partial \boldsymbol{v}}, \tag{121}$$

where Df_1/Dt denotes the total rate of change of f_1 along a set of trajectories in phase space defined by the unperturbed equations of motion:

$$\frac{d\boldsymbol{x}}{dt} = \boldsymbol{v}, \qquad \frac{d\boldsymbol{v}}{dt} = \frac{q}{m}(\boldsymbol{v} \times \boldsymbol{B}_0). \tag{122}$$

In the language of partial differential equations, these trajectories are the *characteristics* of the linearised Vlasov equation. If $f_1 \to 0$ as $t \to -\infty$, it follows immediately from Eq. (121) that

$$f_1(\boldsymbol{x}, \boldsymbol{v}, t) = -\frac{q}{m}\int_{-\infty}^{t} [\boldsymbol{E}_1(\boldsymbol{x}', t') + \boldsymbol{v}' \times \boldsymbol{B}_1(\boldsymbol{x}', t')] \cdot \frac{\partial f_0}{\partial \boldsymbol{v}'} dt', \tag{123}$$

where $\boldsymbol{x}'$, $\boldsymbol{v}'$ denote the position and velocity of a particle at time t' on an unperturbed orbit with position and velocity $\boldsymbol{x}$, $\boldsymbol{v}$ at time t.

Further calculation is required for the formal solution of the Vlasov equation given by Eq. (123) to be of practical use for stability analysis. Following the approach used by Cairns (1985), we will present only an outline of the calculation: more details can be found, for example, in the book by Stix (1992). In principle, the analysis can be applied to any plasma configuration; in practice, however, analytical progress is possible only for very simple equilibria, such as the uniform plasma considered here. In this case we can write

$$x' = x - \frac{v_\perp}{\Omega}\left[\sin\left\{\Omega(t-t') + \alpha\right\} - \sin\alpha\right], \tag{124}$$

$$y' = y + \frac{v_\perp}{\Omega}\left[\cos\left\{\Omega(t-t') + \alpha\right\} - \cos\alpha\right], \tag{125}$$

$$z' = z - v_\parallel(t-t'), \tag{126}$$

where $\Omega = qB_0/m$ is the particle cyclotron frequency in the unperturbed magnetic field. It is straightforward to verify that Eqs. (124-126) are solutions of the unperturbed equations of motion, Eq. (122). Using the fact that f_0 depends only on the constants of the unperturbed motion $v_\parallel$ and $v_\perp$, one can use Eqs. (124-126) to express the components of $\partial f_0/\partial \boldsymbol{v}'$ in terms of $\partial f_0/\partial v_\perp$ and $\partial f_0/\partial v_\parallel$:

$$\frac{\partial f_0}{\partial v_x'} = \cos\{\Omega(t-t') + \alpha\}\frac{\partial f_0}{\partial v_\perp}, \quad \frac{\partial f_0}{\partial v_y'} = \sin\{\Omega(t-t') + \alpha\}\frac{\partial f_0}{\partial v_\perp}, \quad \frac{\partial f_0}{\partial v_z'} = \frac{\partial f_0}{\partial v_\parallel}. \tag{127}$$

For the purpose of evaluating the perturbed distribution function [Eq. (123)], we now consider field perturbations corresponding to waves propagating at an arbitrary angle with respect to $\boldsymbol{B}_0$: without loss of generality, we can choose the wavevector $\boldsymbol{k}$ to lie in the (x, z) plane, so that

$$\boldsymbol{E}_1, \boldsymbol{B}_1 \sim \exp(i\boldsymbol{k} \cdot \boldsymbol{x}' - i\omega t') = \exp(ik_\perp x' + k_\parallel z' - i\omega t'). \tag{128}$$

For field perturbations of this form, the integral in Eq. (123) can be evaluated analytically by making use of the identity (Gradshteyn and Ryzhik 1965)

$$e^{ia\sin x} = \sum_{\ell=-\infty}^{\infty} J_\ell(a) e^{i\ell x}, \tag{129}$$

where J_ℓ is the Bessel function of order ℓ. Applying this expansion to the exponential factors in Eq. (123) yields

$$\exp\left(-\frac{ik_\perp v_\perp}{\Omega}\sin[\Omega(t-t')+\alpha]\right) = \sum_{\ell=-\infty}^{\infty} J_\ell\left(\frac{k_\perp v_\perp}{\Omega}\right)\exp[-i\ell\{\Omega(t-t')+\alpha\}], \tag{130}$$

and

$$\exp\left(\frac{ik_\perp v_\perp}{\Omega}\sin\alpha\right) = \sum_{n=-\infty}^{\infty} J_n\left(\frac{k_\perp v_\perp}{\Omega}\right)\exp(in\alpha), \tag{131}$$

The expressions on the left hand sides of Eqs. (130) and (131) are multiplied together in the integrand appearing in Eq. (123), and thus f_1 can be expressed as a double summation of integrals, all of which can be evaluated analytically since the integrands have only a simple trigonometric dependence on t'. With z' given by Eq. (126), it is apparent that the integration with respect to t' produces denominators of the form $\omega - k_\parallel v_\parallel - \ell\Omega$. The perturbed current can be computed by multiplying f_1 by $\boldsymbol{v}$ and integrating over velocity space. The integration over gyrophase angle α reduces the double summation arising from the use of Eqs. (130) and (131) to a single summation over terms containing products of Bessel functions and their derivatives. This reduction arises from the fact that f_0 is independent of α together with the orthogonality relation

$$\int_0^{2\pi} e^{in\alpha} e^{-i\ell\alpha} d\alpha = 2\pi\delta_{n\ell}, \tag{132}$$

$\delta_{n\ell}$ being the Kronecker delta. Eliminating $\boldsymbol{B}_1$ from the Fourier transforms of Maxwell's equations then yields three linear homogeneous equations for the components $\boldsymbol{E}_1$. Setting the determinant of coefficients in this system of equations equal to zero finally yields a dispersion relation for waves propagating at arbitrary angles with respect to the magnetic field (Krall and Trivelpiece 1986).

If the wave electric field is assumed to be polarised in the plane perpendicular to $\boldsymbol{B}_0$, so that $E_{1z} = 0$, it can be shown that the dispersion relation takes the form

$$\left(\epsilon_{xx} - \frac{k_\parallel^2 c^2}{\omega^2}\right)\left(\epsilon_{xx} - \frac{k^2 c^2}{\omega^2}\right) = -\epsilon_{xy}^2, \tag{132}$$

where c is the speed of light and ϵ_{xx}, ϵ_{xy} and ϵ_{yy} are components of the plasma dielectric tensor given by

$$\epsilon_{xx} = 1 + \sum_s \frac{q_s^2}{m_s \epsilon_0 \omega^2} \sum_{\ell=-\infty}^{\infty} \int \frac{v_\perp \left[(\omega - k_\parallel v_\parallel) \partial f_{0s}/\partial v_\perp + k_\parallel v_\perp \partial f_{0s}/\partial v_\parallel \right]}{\omega - k_\parallel v_\parallel - \ell \Omega_s} \frac{\ell^2 J_\ell^2(a_s)}{a_s^2} d^3v, \tag{134}$$

$$\epsilon_{xy} = -i \sum_s \frac{q_s^2}{m_s \epsilon_0 \omega^2} \sum_{\ell=-\infty}^{\infty} \int \frac{v_\perp \left[(\omega - k_\parallel v_\parallel) \partial f_{0s}/\partial v_\perp + k_\parallel v_\perp \partial f_{0s}/\partial v_\parallel \right]}{\omega - k_\parallel v_\parallel - \ell \Omega_s} \frac{\ell J_\ell(a_s) J_\ell'(a_s)}{a_s} d^3v, \tag{135}$$

$$\epsilon_{yy} = 1 + \sum_s \frac{q_s^2}{m_s \epsilon_0 \omega^2} \sum_{\ell=-\infty}^{\infty} \int \frac{v_\perp \left[(\omega - k_\parallel v_\parallel) \partial f_{0s}/\partial v_\perp + k_\parallel v_\perp \partial f_{0s}/\partial v_\parallel \right]}{\omega - k_\parallel v_\parallel - \ell \Omega_s} J_\ell'^2(a_s) d^3v. \tag{136}$$

Here the first summation is over particle species with charge q_s, mass m_s and cyclotron frequency Ω_s, while the second summation is over cyclotron harmonics, and $a_s = k_\perp v_\perp / \Omega_s = k_\perp \rho_s$ where $\rho_s = v_\perp / \Omega_s$ is particle Larmor radius. The purpose of writing out these expressions in full is to highlight points of comparison with the much simpler one-dimensional, electrostatic case represented by Eq. (109), thereby making it easier to identify the conditions that can give rise to strong instability. The first point to note is that the integrands again appear to contain poles, in this case at values of $v_\parallel$ such that

$$\omega - k_\parallel v_\parallel - \ell \Omega_s = 0. \tag{137}$$

In practice the presence of these apparent singularities does not prevent the integrals from converging, since ω is generally a complex number. However when ω is taken to be the real frequency Eq. (137) defines a set of resonances which play a crucial role in the wave-particle interaction. Resonance occurs because the wave frequency, Doppler-shifted into the rest frame of the particle guiding centre, is either zero ($\ell = 0$) or a harmonic of its natural gyration frequency, Ω_s ($\ell \neq 0$). The $\ell = 0$ case was discussed in the previous subsection, and is referred to as the Čerenkov (or Landau) resonance, while the $\ell \neq 0$ cases are referred to as cyclotron resonances. Depending on the shapes of the unperturbed distributions f_{0s}, the cyclotron resonances can cause either wave damping or instability; damping provides the basis of ion cyclotron resonance heating (ICRH) in tokamak plasmas.

Reversal of the flow of energy in ICRH (absorption of wave energy) can occur if there is some form of population inversion in the ion distribution. As in the Landau resonance case, instability can be driven via the cyclotron resonances by non-Maxwellian particle distributions. For example, fast Alfvén waves with $\omega \simeq k_\perp c_A$ (c_A now being the Alfvén speed of a plasma with uniform equilibrium density) can be excited at frequencies close to ion cyclotron harmonics $\ell \Omega_i$ by ion ring distributions of this type:

$$f_{0s} \sim \exp\left[-\frac{(v_\parallel - v_{\parallel 0})^2}{\delta v_\parallel^2} \right] \delta(v_\perp - v_{\perp 0}), \tag{138}$$

where $v_{\parallel 0}$, $\delta v_\parallel$ and $v_{\perp 0}$ are constants. In principle, instability can occur for any value of the ring velocity $v_{\perp 0}$, since $v_\perp$ does not appear in the resonance condition. However, for

the case of a dilute ion ring distribution embedded in a Maxwellian bulk ion population with the same cyclotron frequency, instability requires $v_{\perp 0}$ to be significantly higher than the bulk ion thermal speed v_{ti}, to avoid strong cyclotron damping. In general $v_{\perp 0}$ also needs to be comparable to or greater than c_A, to ensure that the Bessel function coefficients in the expressions for the dielectric tensor elements are not small (for fast Alfvén waves with $\omega \simeq \ell \Omega_i$, the Bessel function argument a_s is approximately equal to $\ell v_\perp / c_A$, and $J_\ell \propto a_s^\ell$ for small a_s). In many plasmas $c_A \gg v_{ti}$, and an instability of this type can occur if a highly suprathermal ion population with $v_\perp \sim c_A$ is present.

Equation (138) can be used to approximate the local velocity distribution of centrally-born 3.5 MeV fusion α-particles undergoing drift orbit excursions to the outer edge of JET deuterium-tritium plasmas (Cottrell et al. 1993), and also the distribution of energetic protons in equatorial regions of the Earth's radiation belts (Perraut et al. 1982). In both cases *ion cyclotron emission* (ICE) has been detected at frequencies close to multiple harmonics of the energetic ion cyclotron frequency. Similar emission has been detected in many other tokamaks and in the large helical device (LHD) stellarator [for a recent review, see McClements et al. (2015)]. It is generally accepted that these emissions can be attributed to fast Alfvén waves driven by population-inverted fast ions. For plasmas containing a dilute fast ion distribution given by Eq. (138), the dispersion relation Eq. (133) can be solved analytically for the real frequency and growth or damping rate (Dendy et al. 1994). In Fig. 8 the growth rate is plotted versus frequency for obliquely-propagating fast Alfvén waves with $k_\parallel / k = -0.34$ in a hydrogen bulk plasma with ^{3}He fast ions, the ratio of fast ion density to bulk ion density being 1%. The other parameters of the ^{3}He distribution were taken to be $v_{\perp 0}/c_A = 1.5$, $\delta v_\parallel / v_{\perp 0} = 0.1$ and $v_{\parallel 0}/v_{\perp 0} = 0.5$. It can be seen that strong instability (a growth rate equal to several percent of the ^{3}He cyclotron frequency) occurs at frequencies which are somewhat lower than the ^{3}He cyclotron frequency, due to the Doppler shift arising from finite $k_\parallel$ and $v_{\parallel 0}$. This example is relevant to tokamaks, since some ICRH schemes in these devices are designed to preferentially heat minority ion species such as ^{3}He. The highest energy minority ions, typically accelerated close to the plasma centre, can undergo large drift orbit excursions to the outer plasma edge, and thereby excite ICE in the same way as fusion α-particles in deuterium-tritium plasmas (Jacquet et al. 2011).

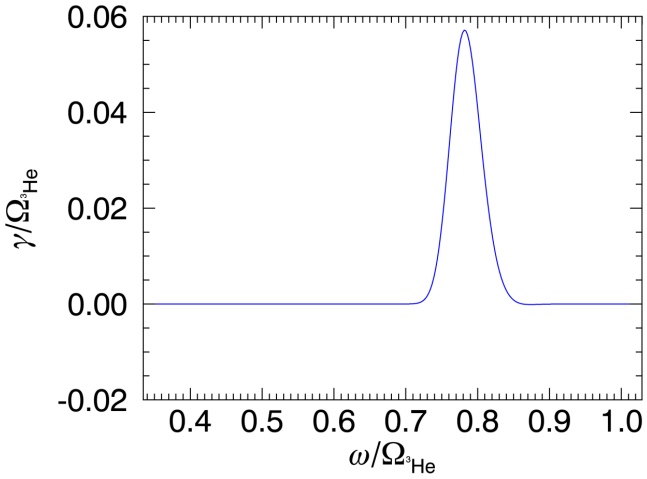

Fig. 8 Linear growth rate versus frequency (both in units of the ^{3}He cyclotron frequency) for fast Alfvén waves in a hydrogen bulk plasma with a ^{3}He fast ion population.

The total power in ICE is typically very small; in the case of the JET preliminary tritium experiment Cottrell et al. (1993) estimated the power to be a few watts, compared to a fusion α-particle power of around 350 kW. However this type of emission can be used as a fast particle diagnostic. It has for example provided evidence that the confinement of fusion α-particles in JET deuterium-tritium pulses was determined mainly by Coulomb collisions (McClements et al. 1999). Self-consistent nonlinear modelling of the ICE instability in full toroidal geometry has yet to be carried out, but Cook et al. (2013) found a close correspondence between the measured ICE spectrum in the JET preliminary tritium experiment and both linear and nonlinear stability calculations carried out in the uniform plasma approximation using local parameters representative of the outer plasma edge in this JET experiment.

Acknowledgments

This work has been part-funded by the EPSRC Fusion Grant 2022/27 [grant number EP/W006839/1]. To obtain further information on the data and models underlying this paper please contact PublicationsManager@ukaea.uk.

References

M Abramowitz and I A Stegun 1965, *Handbook of Mathematical Functions* (New York: Dover)

W H Bennett 1934, *Phys. Rev.* **45**, 890.

H L Berk and B N Breizman 1990, *Phys. Fluids B* **2** 2226.

I B Bernstein, E A Frieman, M D Kruskal and R M Kulsrud 1958, *Proc. Roy. Soc. (London)* **A244**, 17.

O Buneman 1958, *Phys. Rev. Lett.* **1** 8.

I H Cairns and P A Robinson 1999, *Phys. Rev. Lett.* **82** 3066.

R A Cairns 1985, *Plasma Physics* (Blackie: Glasgow).

R Carruthers and P A Davenport 1957, *Proc. Phys. Soc.* **70**, 49.

I T Chapman, J P Graves, T Johnson, O Asunta, P Bonoli, M Choi, E F Jaeger, M Jucker and O Sauter 2011, *Plasma Phys. Control. Fusion* **53**, 124003.

J W S Cook, R O Dendy and S C Chapman 2013, *Plasma Phys. Control. Fusion* **55** 065003.

F F Chen 1984, *Introduction to Plasma Physics and Controlled Fusion Volume 1: Plasma Physics* (Plenum: New York).

J W Connor, R J Hastie and J B Taylor 1978, *Phys. Rev. Lett.* **40** 396.

G A Cottrell, V P Bhatnagar, O da Costa, R O Dendy, J Jacquinot, K G McClements, D C McCune, M F F Nave, P Smeulders and D F H Start 1993, *Nucl. Fusion* **33** 1365.

T G Cowling 1976, *Magnetohydrodynamics* (Bristol: Adam Hilger)

R O Dendy, C N Lashmore-Davies, K G McClements and G A Cottrell 1994, *Phys. Plasmas* **1** 1918.

B D Fried and S D Conte 1961, *The Plasma Dispersion Function: the Hilbert Transform of the Gaussian* (Academic Press: New York).

I S Gradshteyn and I M Ryzhik 1965, *Table of Integrals, Series, and Products* (Academic Press: New York).

A W Hood and E R Priest 1979, *Solar Phys.* **64**, 303.

P Jacquet, G Berger-By, V Bobkov, T Blackman, I E Day, F Durodié, M Graham, T Hellsten, M Laxåback, M-L Mayoral, I Monakhov, M Nightingale, S E Sharapov, M Vrancken and JET-EFDA contributors 2011, *AIP Conf. Proc.* **1406** 17.

B B Kadomtsev 1966, *Rev. Plasma Phys.* **2**, 153.

N A Krall and A W Trivelpiece 1986, *Principles of Plasma Physics* (San Francisco Press: San Francisco).

M D Kruskal 1954, U.S. Atomic Energy Commission Report No. NYO-6015.

L-X Li 2000, *Astrophys. J. Lett.* **531**, L111.

K G McClements, C Hunt, R O Dendy and G A Cottrell 1999, *Phys. Rev. Lett.* **82** 2099.

K G McClements, M E Dieckmann, A Ynnerman, S C Chapman and R O Dendy 2001, *Phys. Rev. lett.* **87** 255002.

K G McClements, R D'Inca, R O Dendy, L Carbajal, S C Chapman, J W S Cook, R W Harvey, W W Heidbrink and S D Pinches 2015, *Nucl. Fusion* **55** 043013.

P McQuillan and K G McClements 1988, *J. Plasma Phys.* **40** 493.

Y Omura, H Matsumoto, T Miyake and H Kojima 1996, *J. Geophys. Res.* **101** 2685.

M Oppenheim, N Otani and C Ronchi 1996, *J. Geophys. Res.* **101** 17,273.

D J Pascoe, V M Nakariakov and T D Arber 2007, *Solar Phys.* **246**, 165.

S Perraut, A Roux, P Robert, R Gendrin, J-A Sauvaud, J-M Bosqued, G Kremser and A Korth 1982, *J. Geophys. Res.* **87** 6219.

Lord Rayleigh 1883, *Proc. London Math. Soc.* **14**, 170.

B A Remington, J Kane, R P Drake, S G Glendinning, K Estabrook, R London, J Castor, R J Wallace, D Arnett, E Liang, R McCray, A Rubenchik and B Fryxell 1997, *Phys. Plasmas* **4**, 1994.

P A Robinson and I H Cairns 1998, *Solar Phys.* **181** 363.

M J Schaffer, J E Menard, M P Aldan, J M Bialek, T E Evans and R A Moyer 2008, *Nucl. Fusion* **48** 024004.

V D Shafranov 1957, *J. Nuc. Energy III* **5**, 86.

J N Shiau, E B Goldman and C I Weng 1974, *Phys. Rev. Lett.* **32**, 352.

P B Snyder, H R Wilson, J R Ferron, L L Lao, A W Leonard, T H Osborne, A D Turnbull, D Mossessian, M Murakami, X Q Xu 2002, *Phys. Plasmas* **9** 2037.

T H Stix 1992, *Waves in Plasmas* (American Institute of Physics: New York).

Y Takeda and K Yamagiwa 1985, *Phys. Rev. Lett.* **55** 711.

A Thyagaraja and K G McClements 2009, *Phys. Plasmas* **16**, 092506.

V V Vikhrev, V V Ivanov and G A Rozanova 1993, *Nucl. Fusion* **33**, 311.

J Wesson 2004, *Tokamaks* third edition (Oxford University Press: Oxford).

J Wesson 2015, *Phys. Plasmas* **22** 022519.